

Geophysically-derived temperature and crystal fabric constrain past and present ice-sheet dynamics

Overview. The greatest uncertainty for projections of future sea-level rise is ice-sheet dynamics and the potential realization of theorized instabilities (Fox-Kemper et al., 2021). While knowledge on the precise fate of Earth's ice sheets is still out of reach, looking to past states could provide insight on their potential evolution. Past ice-sheet states and particularly their dynamics are preserved in present-day ice temperature (Robin, 1955) and preferred crystal orientation fabric (COF) (Alley, 1988); moreover, the future ice dynamics are governed by those same properties through the ice viscosity (Azuma, 1994; Glen, 1955) and ice sliding over a temperate bed (Lliboutry, 1968; Weertman, 1957). Theoretically, ice temperature and COF can both be measured using the amplitude and phase information from a reflected radar wave (MacGregor et al., 2007; Matsuoka et al., 2009), but prior work shows that it is difficult to disentangle these intrinsic properties of the ice column from each other or even from interface properties, such as reflectivity between layers and at the ice-sheet bed (e.g. Holschuh et al., 2016). Here, I outline my proposal which contributes to the incremental development of methods for radar power and phase interpretation, and to use those methods alongside process models to infer both present-day and paleo ice-sheet dynamics. I focus on three regions of the Antarctic Ice Sheet: the Siple Coast, South Pole Lake, and Hercules Dome, with the specific scientific problem being different for each.

1. Background

Ice-sheet history is commonly inferred using numerical models (DeConto and Pollard, 2016), using proxies from the underlying geology (Brook et al., 1996) and sediment (Venturelli et al., 2020), and using ice stratigraphy as surveyed with geophysical tools (MacGregor et al., 2015a). Direct measurements of physical properties from ice cores, as opposed to proxy records, have also been used to infer ice-sheet history including borehole thermometry (Dahl-Jensen et al., 1998) and thin sections of the COF (Alley, 1988). Here, I focus on how those physical properties can be inferred remotely with ice-penetrating radar and what can be learned about ice-sheet history without direct sampling or in-situ instrumentation. In this section, I overview the current glaciological theory for both ice temperature and COF. Then, I discuss the influence each has on the electrical properties of ice and how they can be measured remotely using ice-penetrating radar.

1.1 Ice Temperature

Temperatures of glacier ice range from the melting point to $\sim -60^{\circ}\text{C}$, which corresponds to a viscosity range over three orders of magnitude (Glen, 1955). Ice is generally warmest at the glacier bed, being heated from below by the geothermal flux, and coldest near the surface where ice is in equilibrium with the mean air temperature. Heat transfer between those two boundaries is an advection-diffusion problem with heat generation by strain (Clarke et al., 1977) and, in some cases, liquid water infiltration (Phillips et al., 2010). Because the length scale for thermal diffusion in ice is long, deviations in ice temperature can be preserved for thousands of years (Figure 1A).

Near an ice divide, there are few heat sources and advection is predominantly vertical with a velocity profile that is relatively well understood (Lliboutry, 1979). Therefore, strong inferences can be made for the unknown parameters at the boundaries. For

instance, climate history is inferred using borehole thermometry (Dahl-Jensen et al., 1998), and geothermal flux is constrained at locations where the thermal state of the bed is known to be either frozen or thawed (Fudge et al., 2019).

Away from the ice divide, flow speeds generally increase, which results in more strain heating, and longitudinal and lateral advection affect ice temperature more. Longitudinal advection is generally under-appreciated in simple temperature models (c.f. Dahl-Jensen, 1998; Weertman, 1968), but it has been observed in locations with fast flow and a strong surface temperature gradient (e.g. Harrington et al., 2015; Iken et al., 1993). Lateral advection is important along ice-stream shear margins, where there are typically strong lateral temperature gradients. Theory on shear-margin temperature comes from a few isolated measurements in the Siple Coast ice streams (Engelhardt, 2004) as well as thermodynamic models of varying complexity (Jacobson and Raymond, 1998; Meyer and Minchew, 2018; Perol and Rice, 2015; Suckale et al., 2014). Despite the efforts to increase theoretical understanding, these models are likely still underestimating the importance of both vertical (Holschuh et al., 2019) and longitudinal advection.

1.2 Crystal Orientation Fabric

Snow crystals are deposited at random orientation on the glacier surface, resulting in an initially isotropic COF. As ice flows, crystal c-axes rotate away from the primary extensional axis and toward compression (Figure 1B) (Alley, 1992). Single-pole fabrics with upward-pointing c-axes develop at an ice dome where flow is by uniform vertical compression and outward extension in all directions from the dome. In this case, the ice hardens in the vertical and old ice is preserved near the bed (Raymond, 1983). Along an ice divide, where there is one prominent extensional direction, a vertical girdle develops perpendicular to the axis of extension (Young et al., 2021). The center of an ice-stream is

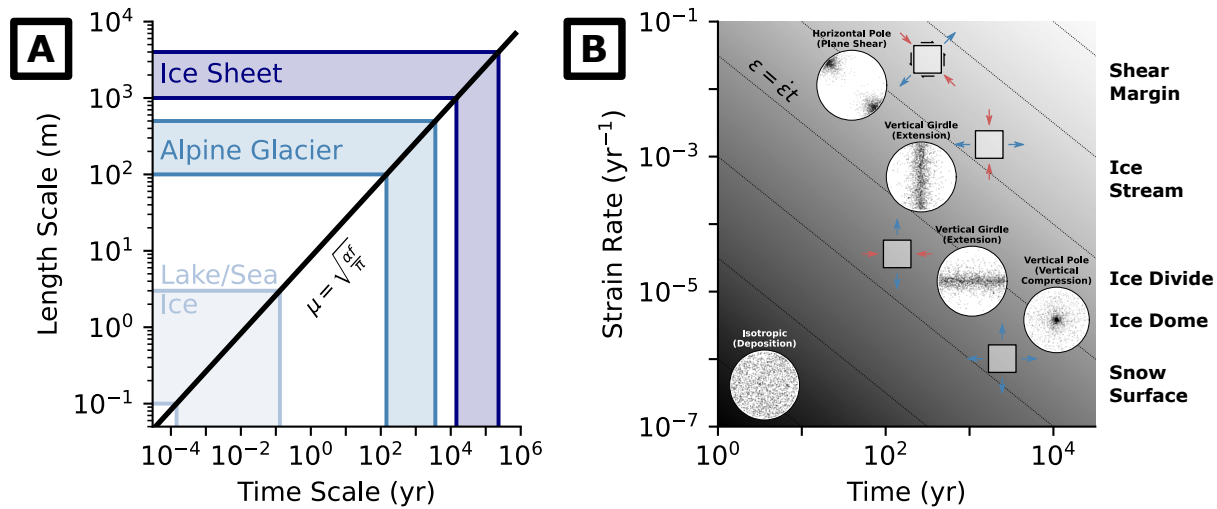


Figure 1. Relevant process timescales in ice. A) The characteristic length scale for thermal diffusion, μ , is dependent on the temporal frequency of the temperature change, f , and the thermal diffusivity of ice, α . B) Crystal reorientation is a result of cumulative strain, $\epsilon = \dot{\epsilon}t$, so the quality and strength of a crystal fabric depend on the spatial pattern of local strain rates and the total time over which those have been stable.

similar, with extension in the direction of ice flow (Smith et al., 2017). A partial horizontal girdle develops in an ice-stream shear margin where transverse shear dominates.

The COF strength depends on the total strain accumulated over time. Laboratory studies show that cumulative crystal reorientation is sufficient to effect subsequent deformation by cumulative strain $\sim 0.1\text{-}0.15$ (Budd and Jacka, 1989). Therefore, vertical strain rates at an ice dome or ice divide, $\sim 10^{-5}\text{-}10^{-4}$ yr $^{-1}$, would develop a recognizable COF on the order of thousands to tens of thousands of years. In areas with much higher strain rates such as an ice-stream shear margin, $\sim 10^{-2}\text{-}10^{-1}$ yr $^{-1}$, the COF develops much faster, even on the order of years. An established COF in a shear margin can further soften the ice and promote faster flow (Jackson and Kamb, 1997), with ice being up to two orders of magnitude softer depending on crystal orientation (Shoji and Langway, 1988).

1.3 Radar Power and Phase Interpretation

Theoretically, ice temperature and COF can both be measured without drilling into the ice by interpreting their effect on the measured power (attenuation) and phase (birefringence) from ice-penetrating radar. Radio waves are attenuated in ice primarily by electrical conduction. Protons are the charge carrier in ice, so conduction is facilitated by the movement of protonic defects in an imposed electric field (Figure 2A). As a radar wave propagates through the crystal, its power is attenuated more if proton conduction is more efficient; that is, if there are more free charge carriers (more ions), adequate lattice positions to accommodate charge conduction (more defects), or more energy available for molecular rotations (higher temperatures). Ice chemistry (ions) and defects are only spatially variable over the broad synoptic scale ($>100\text{s km}^2$), so any measurable change in radar attenuation at the \sim mesoscale (10s to 100s km 2) is most likely associated with contrasts in ice temperature (e.g. MacGregor et al., 2015b; Schroeder et al., 2016).

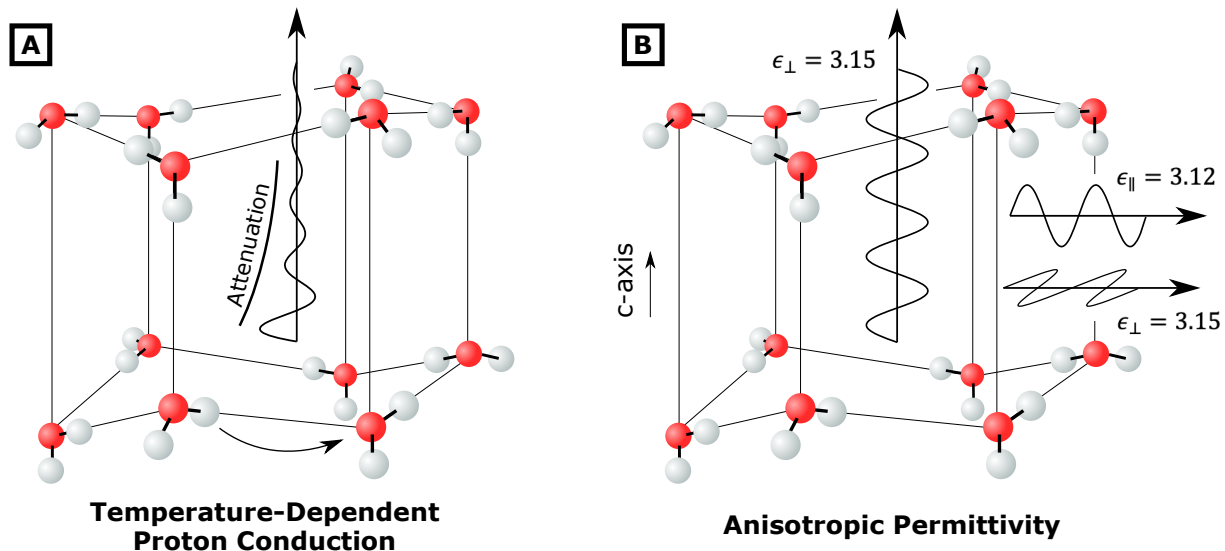


Figure 2. An illustration of radar attenuation (A) and crystal anisotropy (B) at the molecular scale. Protons (white spheres) move between molecules in an imposed electric field. Electromagnetic wave speeds ($\frac{1}{\sqrt{\epsilon}}$) are slightly faster when polarized parallel (ϵ_{\parallel}) to the c-axis than perpendicular (ϵ_{\perp}).

Ice permittivity is anisotropic (Fujita et al., 2000). Radio waves propagate fastest when their polarization aligns with the crystal c-axis (Figure 2B). Bulk permittivity is thus dependent on the aggregate orientation of ice crystals (the COF) and the wave polarization relative to that COF. For instance, a girdle fabric induces a measurable phase delay between radar acquisitions polarized parallel vs. perpendicular to the girdle, with the magnitude of the phase gradient correlating to the strength of the girdle (Jordan et al., 2020). When polarized oblique to the girdle, the wave ‘turns’ as it propagates through the ice. That is, an initially linearly polarized wave transitions to circular (or elliptic) polarization. The instrument orientation at which no ‘turn’ is observed (cross-polarized extinction) can then be assumed to align with the girdle orientation (Ershadi et al., 2021). In theory, wave reflection properties (scattering) can also be anisotropic (Drews et al., 2012), possibly causing an abrupt phase transition in the received waveform. Below, I focus on steady phase gradients which should be minimally affected by anisotropic scatterers.

For each of the scientific studies that I propose, I leverage the theory presented above on the electrical properties of ice to interpret ice-penetrating radar measurements and infer ice properties. I use those radar-derived constraints on ice properties along with process models to interpret past and present ice-sheet flow.

2. Proposed Projects

In what follows, I describe the work that I have done up to now on methods development as well as three proposed scientific investigations which apply those methods. Each of the proposed projects has at least some preliminary results, with the first two being significantly more developed (one published and one ready to submit) than the third.

2.1 Methods Development

Deliverables: One lead-author (*Hills et al., 2020*) and one coauthor manuscript (*Lilien et al., 2020*)

Within the glaciology community, there is no consistent radar processing methodology and implementation strategy. Data processed by different groups are not easily comparable. In an effort to standardize processing, we created ImpDAR (Lilien et al., 2020), a free, open-source, and pip-installable Python radar processing library. ImpDAR is compatible with many of the commercial radar systems, including PulseEKKO, GSSI, RAMAC, as well as some custom data formats, such as the Gecko software used for high-frequency impulse radar systems (e.g. Welch and Jacobel, 2005). Within ImpDAR, we are building the tools for power and phase interpretation. A framework for empirical attenuation measurements was designed by Hills et al. (2020) and all methods are included in ImpDAR. Processing flows for Autonomous phase-sensitive Radio Echo Sounding (ApRES) measurements (Nicholls et al., 2015) of both vertical motion (Brennan et al., 2014) and polarimetry (Jordan et al., 2019) are also being added to ImpDAR.

2.2. Study 1 – Siple Coast Ice Streams

Deliverables: One lead-author manuscript (*Hills et al., in review*)

Recent studies suggest that plane-shear strain in ice-stream shear margins may warm ice to its melting temperature through as much as half of the ice column (Meyer and Minchew, 2018; Perol and Rice, 2015). This excessively warm ice is necessary to match the high strain rates from observed surface velocities (Suckale et al., 2014). However, in-situ measurements of ice temperature from hot-water boreholes (Engelhardt, 2004) and

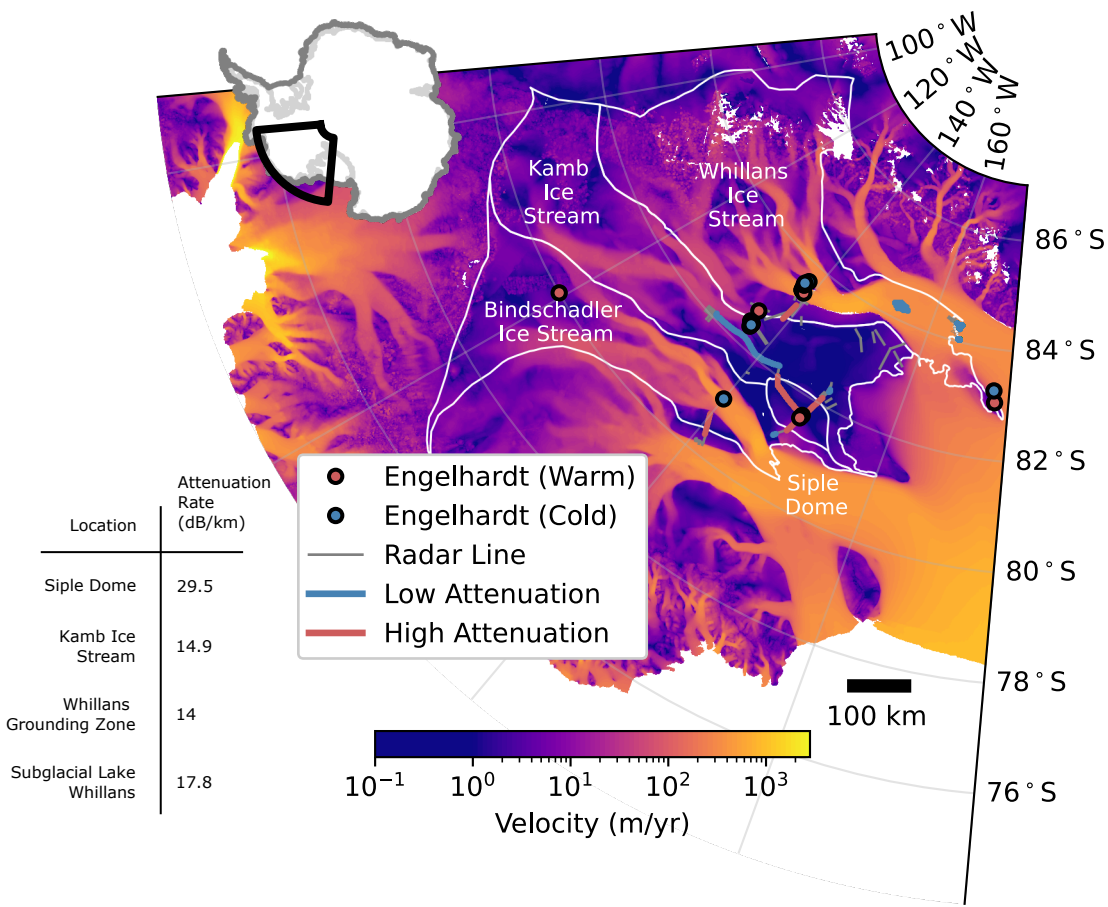


Figure 3. Data and radar analysis summary of Study 1 – Siple Coast Ice Streams. The colormap shows ice surface velocity (Mouginot et al., 2019). Dots mark borehole drilling locations colored to indicate whether the measured temperature profile is relatively cold (blue) or warm (red) based on the original distinction (Engelhardt, 2004). Lines correspond to the radar profiles collected in previous studies. Drainage areas of the Bindschadler, Kamb, and Whillans ice streams are outlined in white (Rignot et al., 2013), as is Siple Dome. Table) Attenuation rates from previously published ground-based radar studies in this region.

inferred ice temperature from radar attenuation (Figure 3) (Christianson et al., 2016, 2012; Jacobel et al., 2009) each independently suggest that temperature in the Siple Coast Ice Streams is in fact *colder* than the surrounding slow-flowing ridges. Even measurements directly from the Dragon Shear Margin of Whillans Ice Stream (Harrison et al., 1998) are $\sim 10^\circ\text{C}$ colder than suggested by the analytical solution for shear-margin temperature (Meyer and Minchew, 2018).

Hypothesis: Longitudinal temperature gradients in the Siple Coast ice streams are a sufficiently strong advective heat sink to compete with heat production in the shear margins. An alternative weakening mechanism is required to match the measured strain rates.

I propose a two-prong approach to address ice-stream and shear-margin temperatures throughout the Siple Coast Ice Streams. First, I summarize the attenuation calculations from prior ground-based radar surveys (e.g. Christianson et al., 2016; Gades et al., 2000;

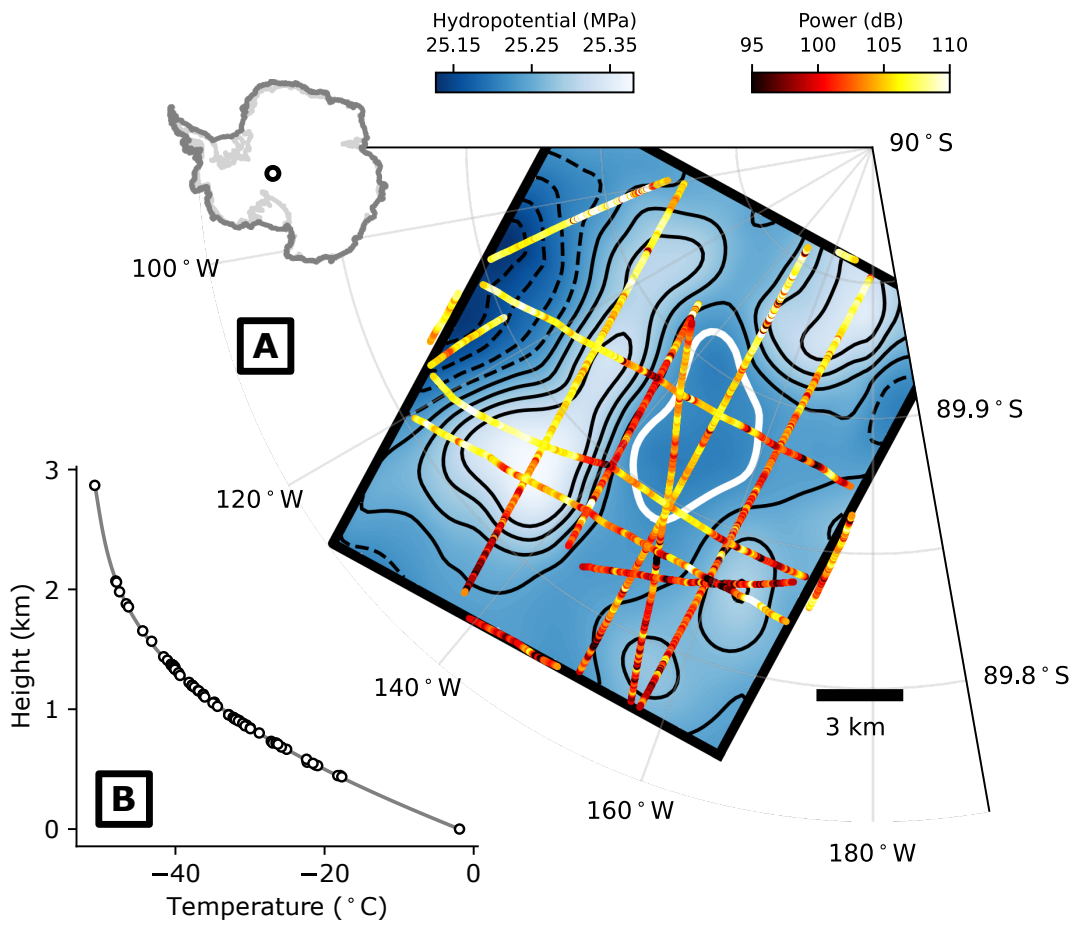


Figure 4: Data and model summary of Study 2 – South Pole Lake. A) Map of SPL survey with the colormap and black contours showing hydropotential and the white outline showing the lake area inferred by a hydropotential basin. Colored lines are the measured bed-echo power from an ice-penetrating radar. B) Measured (Price et al., 2002) and modeled (grey line) temperature profiles.

Jacobel et al., 2009), applying various methods from the framework we developed for empirical attenuation (Hills et al., 2020). While these attenuation results have been presented in past studies, they have been used solely in the context of a local interpretation or as a correction to bed-reflectivity analysis. Second, I add a longitudinal advection parameterization to the standard advection-diffusion thermal model. I use this model to directly compare the amplitude of the advective heat sink to in-situ heat generation from vertical shear near the ice-bed interface and plane shear in the lateral shear margins. I use standard data products to calculate longitudinal advection for three ice-stream catchments (Figure 3) and compare the model result to borehole temperature measurements (Engelhardt, 2004; Harrison et al., 1998).

2.3. Study 2 – South Pole Lake

Deliverables: One lead-author manuscript (Hills et al., 2022)

The history of ice-sheet dynamics in the South Pole sector through the glacial transition are actively debated. Temperature measurements from the AMANDA and IceCube projects

(Price et al., 2002) were interpreted to suggest that the deep ice is too cold for a thawed bed despite prior airborne radar observations of the nearby South Pole Lake (SPL) (Carter et al., 2007). Price et al. (2002) suggested that the lake had completely frozen and that the observations were a ‘fossil’ of the prior ice sheet. While active-source seismics have since confirmed that the lake persists today (Peters et al., 2008), Beem et al. (2017) argued that the presence of liquid water is not incompatible with the cold temperature measurements. They posited that the lake was created during the last glacial period (~14 thousand years ago) when the Support Force Ice Stream extended into this region, sufficiently increasing heat production and basal melt to form the lake. Their interpretation of a paleo ice stream is consistent with prior radar interpretations of submergence rates (Beem et al., 2017) and internal layer disruptions (Bingham et al., 2007). A secondary theory for South Pole dynamics contradicts the first. Lilien et al. (2018) compared historical accumulation rates collected from the South Pole Ice Core to accumulation rates from an upstream radar survey and found that ice thickened and sped up through the Holocene.

Hypothesis: The South Pole region of interior East Antarctica is thermodynamically stable in the present-day ice dynamic regime and has been through at least the last interglacial. South Pole Lake is therefore a viable target for subglacial sediment sampling.

For this study, we took an integrated approach that interprets historical thermodynamics and the present-day ice dynamics together. Prior studies did not use historical data to constrain temperature modeling, but newly available data from the South Pole Ice Core make this possible. We use accumulation and temperature proxy data from the ice core (Kahle et al., 2021) as boundary conditions for a 1.5-dimensional model of ice temperature through time (*model from Study 1*). We then optimize the modeled geothermal flux so that the output most closely matches present-day ice temperature measurements from IceCube (Price et al., 2002) and a temperate bed for the measured ice thickness, assuming regional basal melt.

In addition to the temperature modeling, we have conducted the most comprehensive geophysical survey to date of SPL (Figure 4) to understand its present-day dynamic setting, which also provides a constraint on the thermodynamic history. We mapped the surface elevation using kinematic GNSS, mapped the ice stratigraphy and ice thickness using deep-sounding radar, measured vertical ice motion at 10 locations on and off the lake using ApRES, and measured horizontal ice motion at 50 locations on and off the lake using precision GPS. We find that the lake is currently full to its capacity, implying that significant basal freeze-on through the Holocene is unlikely. Our horizontal and vertical strain measurements also indicate that basal sliding is likely occurring today, consistent with a regionally thawed bed.

2.4. Study 3 – Hercules Dome

Deliverables: One lead-author manuscript (targeting TC or JGR) and various coauthors

Hercules Dome (HD) lies in the bottleneck between the East and West Antarctic Ice Sheet (WAIS). It is sufficiently proximal to the WAIS that an isotopic record of hypothetical WAIS collapse during the last interglacial period (~120 ka) could be preserved in the deepest ice (Steig et al., 2015). In a recent study, we demonstrated high likelihood that ice from the last interglacial period is preserved at the grid-westernmost extent of HD with signs of a frozen bed and stable divide flow, including a Raymond effect (Fudge et al., in prep). However, it is not clear how past transitions in ice flow and divide migration may

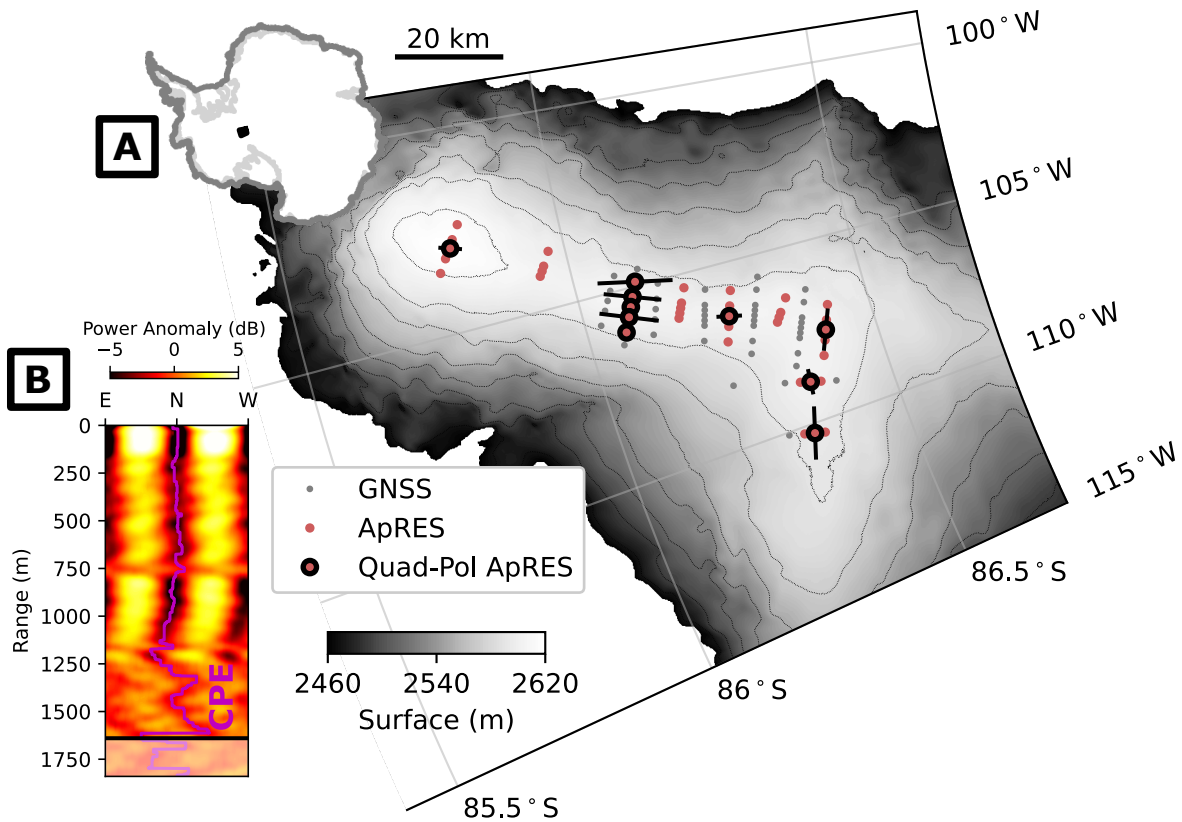


Figure 5: Data and radar analysis summary of Study 3 – Hercules Dome. A) Map of the HD survey with the colormap showing surface elevation from REMA (Howat et al., 2019), GNSS (grey), single-pol ApRES sites (red), and quad-pol ApRES sites (red with black bars at the inferred girdle axis). B) Cross-polarized power anomaly from one site with the cross-polarized extinction (CPE; magenta) being oriented in line with the girdle axis.

affect ice-core interpretation. This is made especially clear by evidence of past streaming flow preserved in bedrock troughs beneath the grid-eastern portions of HD (Hoffman et al., in prep).

Hypothesis: *The present-day surface geometry of Hercules Dome, a triple divide, is consistent with historical ice dynamics at least since the last glacial maximum, and cumulative strain during those ~15-25 ka is preserved in the present-day COF.*

I propose a survey of quad-polarized (quad-pol) ApRES acquisitions at HD with the intent to survey the dome's COF for past and present flow patterns. Unlike multi-polarization methods (e.g. Jordan et al., 2020) which use a series of co-polarized acquisitions at varying azimuth, quad-pol acquisitions use the cross-polarized terms in a rotational transform (Young et al., 2021). Therefore, the orientation and magnitude of a girdle fabric can be isolated by cross-polarized extinction and co-polarized phase delay, respectively.

During the 18-19, 19-20, and 21-22 HD seasons, we conducted quad-pol acquisitions at a total of ten sites which form an 80-kilometer transect along the predominant E-W divide ridge, a 10-kilometer transect which crosses the divide, and two acquisitions on the south

ridge extension (Figure 5). At each acquisition location, the quad-pol data will be translated to depth profiles of x-y COF orientation and strength by optimizing to a layered effective-medium model (Ershadi et al., 2021). The resulting COF orientation and strength profiles across the dome will be interpreted in the context of the present-day surface strain rates measured with repeat GNSS acquisitions and vertical strain rates measured with repeat ApRES acquisitions. The consistency, or lack thereof, between COF results and present-day ice dynamics will be used to investigate the likelihood of divide migration through time.

3. Summary and Outlook

Through the first half of my PhD, I built knowledge on glacier thermodynamics, ice physics, and radar theory. Much of my research has been dedicated toward developing tools for radar processing. In the remainder of my PhD, I will apply those tools to the three scientific problems laid out above. For *Study 1 – Siple Coast*, no new data are needed, the analysis is finished, and the manuscript is ready to submit for review. For *Study 2 – SPL*, all of the data have already been collected and archived, and the manuscript has already been accepted and published. For *Study 3 – HD*, the necessary data have been collected and initial analysis has been done. Near-term objectives are to develop the effective medium model and constrain depth profiles of COF orientation and strength at each quad-pol location. This project will be completed after the next field season ('22-'23) when the repeat ApRES acquisitions for vertical velocity can be made at all locations.

Supplementary Work: One lead-author letter on numerical modeling of the Stefan Problem in cylindrical coordinates to aid design of a thermal melt probe (Hills et al., 2021).

Data and Code Availability: Data products will be made available through the UW Research Archive and USAP Data Center. The data from SPL have been archived, <https://www.usap-dc.org/view/project/p0010160>. Hercules Dome data will be archived with USAP-DC as well. Processing and modeling code are available at <https://github.com/benhillis>.

Funding: Funding from NSF grants 1744649 and 1643353 as well as NASA grant NNX17AF68G. I will continue to be funded on grant 1744649 and possibly others.

References

- Alley, R.B., 1992. Flow-law hypotheses for ice-sheet modeling. *J. Glaciol.* 38.
- Alley, R.B., 1988. Fabrics in Polar Ice Sheets: Development and Prediction. *Science* (80-). 240, 493–495.
- Azuma, N., 1994. A flow law for anisotropic ice and its application to ice sheets. *Earth Planet. Sci. Lett.* 128, 601–614. [https://doi.org/10.1016/0012-821X\(94\)90173-2](https://doi.org/10.1016/0012-821X(94)90173-2)
- Beem, L.H., Cavitte, M.G.P., Blankenship, D.D., Carter, S.P., Young, D.A., Muldoon, G.R., Jackson, C.S., Siegert, M.J., 2017. Ice-flow reorganization within the East Antarctic Ice Sheet deep interior. *Geol. Soc. London Spec. Publ.* 461. <https://doi.org/10.1144/SP461.14>
- Bingham, R.G., Siegert, M.J., Young, D.A., Blankenship, D.D., 2007. Organized flow from the South Pole to the Filchner-Ronne ice shelf: An assessment of balance velocities in interior East Antarctica using radio echo sounding data. *J. Geophys. Res. Earth Surf.* 112, 1–11. <https://doi.org/10.1029/2006JF000556>
- Brennan, P. V., Lok, L.B., Nicholls, K., Corr, H., 2014. Phase-sensitive FMCW radar system for high-precision antarctic ice shelf profile monitoring. *IET Radar, Sonar Navig.* 8, 776–786. <https://doi.org/10.1049/iet-rsn.2013.0053>
- Brook, E.J., Nesje, A., Lehman, S.J., Raisbeck, G.M., Yiou, F., 1996. Cosmogenic nuclide exposure ages along a vertical transect in western Norway: Implications for the height of the Fennoscandian ice sheet. *Geology* 24, 207–210. [https://doi.org/10.1130/0091-7613\(1996\)024<0207:CNEAAA>2.3.CO;2](https://doi.org/10.1130/0091-7613(1996)024<0207:CNEAAA>2.3.CO;2)
- Budd, W.F., Jacka, T.H., 1989. A review of ice rheology for ice sheet modelling.
- Carter, S.P., Blankenship, D.D., Peters, M.E., Young, D.A., Holt, J.W., Morse, D.L., 2007. Radar-based subglacial lake classification in Antarctica. *Geochemistry Geophys. Geosystems* 8, 1–20. <https://doi.org/10.1029/2006GC001408>
- Christianson, K., Jacobel, R.W., Horgan, H.J., Alley, R.B., Anandakrishnan, S., Holland, D.M., Dallasanta, K.J., 2016. Basal conditions at the grounding zone of Whillans Ice Stream, West Antarctica, from ice-penetrating radar. *J. Geophys. Res. Earth Surf.* 121, 1954–1983. <https://doi.org/10.1002/2015JF003806>
- Christianson, K., Jacobel, R.W., Horgan, H.J., Anandakrishnan, S., Alley, R.B., 2012. Subglacial Lake Whillans - Ice-penetrating radar and GPS observations of a shallow active reservoir beneath a West Antarctic ice stream. *Earth Planet. Sci. Lett.* 331–332, 237–245. <https://doi.org/10.1016/j.epsl.2012.03.013>
- Clarke, G.K.C., Nitsan, U., Paterson, W.S.B., 1977. Strain heating and creep instability in glaciers and ice sheets. *Rev. Geophys.* 15, 235. <https://doi.org/10.1029/RG015i002p00235>
- Dahl-Jensen, D., 1998. Steady thermomechanical flow along two-dimensional flow lines in large grounded ice sheets. *J. Geophys. Res.* 94, 355–362.
- Dahl-Jensen, D., Mosegaard, K., Gundestrup, N., Clow, G.D., Johnsen, S.J., Hansen, A.W., Balling, N., 1998. Past temperatures directly from the Greenland Ice Sheet. *Science* (80-). 282, 268–271. <https://doi.org/10.1126/science.282.5387.268>
- DeConto, R.M., Pollard, D., 2016. Contribution of Antarctica to past and future sea-level rise. *Nature* 531, 591–597. <https://doi.org/10.1038/nature17145>
- Drews, R., Eisen, O., Steinhage, D., Weikusat, I., Kipfstuhl, S., Wilhelms, F., 2012. Potential mechanisms for anisotropy in ice-penetrating radar data. *J. Glaciol.* 58, 613–624. <https://doi.org/10.3189/2012JoG11J114>
- Engelhardt, H., 2004. Thermal regime and dynamics of the West Antarctic ice sheet. *Ann. Glaciol.* Vol 39, 2005 39, 85–92.
- Ershadi, M.R., Drews, R., Martín, C., Eisen, O., Ritz, C., Corr, H., Christmann, J., Zeising, O., Humbert, A., Mulvaney, R., 2021. Polarimetric radar reveals the spatial distribution of ice fabric at domes in East Antarctica. *Cryosph. Discuss.* 1–34.
- Fox-Kemper, B., Hewitt, H.T., Xiao, C., Aðalgeirsdóttir, G., Drijfhout, S.S., Edwards, T.L., Golledge, N.R., Hemer, M., Kopp, R.E., Krinner, G., Mix, A., Notz, D., Nowicki, S., Nurhati, I.S., Ruiz, L., Sallée, J.-B., Slangen, A.B.A., Yu, Y., 2021. Ocean, Cryosphere and Sea Level Change Climate Change 2021: The Physical Science Basis. *Contrib. Work. Gr. I to Sixth Assess. Rep. Panel Clim. Chang.*
- Fudge, T.J., Biyani, S.C., Clemens-Sewall, D., Hawley, R.L., 2019. Constraining Geothermal Flux at Coastal Domes of the Ross Ice Sheet, Antarctica. *Geophys. Res. Lett.* 46, 13090–13098. <https://doi.org/10.1029/2019GL084332>
- Fujita, S., Matsuoka, T., Ishida, T., Matsuoka, K., Mae, S., 2000. A summary of the complex dielectric permittivity of ice in the megahertz range and its applications for radar sounding of polar ice sheets. *Phys. Ice Core Rec.* 185–212.
- Gades, A.M., Raymond, C.F., Conway, H., Jacobel, R.W., 2000. Bed properties of Siple Dome and adjacent ice streams, West

- Antarctica, inferred from radio-echo sounding measurements. *J. Glaciol.* 46, 88–94.
<https://doi.org/10.3189/172756500781833467>
- Glen, J.W., 1955. the Creep of Polycrystalline Ice. *Proc. R. Soc. London A Math. Phys. Eng. Sci.* 228, 519–538.
- Harrington, J. a, Humphrey, N.F., Harper, J.T., 2015. Temperature distribution and thermal anomalies along a flowline of the Greenland Ice Sheet. *Ann. Glaciol.* 56, 98–104. <https://doi.org/10.3189/2015AoG70A945>
- Harrison, W.D., Echelmeyer, K.A., Larsen, C.F., 1998. Measurement of temperature in a margin of Ice Stream B, Antarctica: implications for margin migration and lateral drag. *J. Glaciol.* 44, 615–624.
- Hills, B.H., Christianson, K., Holschuh, N., *in review*. Radar attenuation demonstrates advective cooling at the Siple Coast ice streams. *Journal of Glaciology*.
- Hills, B.H., Christianson, K., Hoffman, A.O., Fudge, T.J., Holschuh, N., Kahle, E.C., Conway, H., Christian, J.E., Horlings, A.N., O'Connor, G.K., Steig, E.J., 2022. Geophysics and Thermodynamics at South Pole Lake Indicate Stability and a Regionally Thawed Bed. *Geophys. Res. Lett.* 49, 1–10. <https://doi.org/10.1029/2021GL096218>
- Hills, B.H., Christianson, K., Holschuh, N., 2020. A framework for attenuation method selection evaluated with ice-penetrating radar data at South Pole Lake. *Ann. Glaciol.* 61, 1–12. <https://doi.org/10.1017/aog.2020.32>
- Hills, B.H., Winebrenner, D.P., Elam, W.T., Kintner, P.M.S., 2021. Avoiding slush for hot-point drilling of glacier boreholes. *Ann. Glaciol.* 62, 166–170. <https://doi.org/10.1017/aog.2020.70>
- Holschuh, N., Christianson, K., Anandakrishnan, S., Alley, R.B., Jacobel, R.W., 2016. Constraining attenuation uncertainty in common midpoint radar surveys of ice sheets. *J. Geophys. Res. F Earth Surf.* 121, 1876–1890.
<https://doi.org/10.1002/2016JF003942>
- Holschuh, N., Lilien, D.A., Christianson, K., 2019. Thermal Weakening, Convergent Flow, and Vertical Heat Transport in the Northeast Greenland Ice Stream Shear Margins. *Geophys. Res. Lett.* 8184–8193.
<https://doi.org/10.1029/2019gl083436>
- Howat, I.M., Porter, C., Smith, B.E., Noh, M.-J., Morin, P., 2019. The Reference Elevation Model of Antarctica. *Cryosph.* 1–16.
<https://doi.org/10.5194/tc-2018-240>
- Iken, A., Echelmeyer, K., Harrison, W., Funk, M., 1993. Mechanisms of fast flow in Jakobshavn Isbrae, West Greenland: Part I. Measurements of temperature and water level in deep boreholes. *J. Glaciol.* 39, 15–25.
- Jackson, M., Kamb, B., 1997. The marginal shear stress of Ice Stream B, West Antarctica. *J. Glaciol.* 43, 415–426.
- Jacobel, R.W., Welch, B.C., Osterhouse, D., Pettersson, R., Macgregor, J.A., 2009. Spatial variation of radar-derived basal conditions on Kamb Ice Stream, West Antarctica. *Ann. Glaciol.* 50, 10–16.
<https://doi.org/10.3189/172756409789097504>
- Jacobson, H.P., Raymond, C.F., 1998. Thermal effects on the location of ice stream margins. *J. Geophys. Res.* 103.
<https://doi.org/10.1029/98JB00574>
- Jordan, T.M., Schroeder, D.M., Castelletti, D., Li, J., Dall, J., 2019. A Polarimetric Coherence Method to Determine Ice Crystal Orientation Fabric from Radar Sounding: Application to the NEEM Ice Core Region. *IEEE Trans. Geosci. Remote Sens.* 57, 8641–8657. <https://doi.org/10.1109/TGRS.2019.2921980>
- Jordan, T.M., Schroeder, D.M., Cooper, W., Siegfried, M.R., 2020. Estimation of ice fabric within Whillans Ice Stream using polarimetric phase-sensitive radar sounding 00, 1–24.
- Kahle, E.C., Steig, E.J., Jones, T.R., Fudge, T.J., Koutnik, M.R., Morris, V.A., Vaughn, B.H., Schauer, A.J., Stevens, C.M., Conway, H., Waddington, E.D., Buizert, C., Epifanio, J., White, J.W.C., 2021. Reconstruction of Temperature, Accumulation Rate, and Layer Thinning From an Ice Core at South Pole, Using a Statistical Inverse Method. *J. Geophys. Res. Atmos.* 126, 1–20. <https://doi.org/10.1029/2020jd033300>
- Lilien, D.A., Fudge, T.J., Koutnik, M.R., Conway, H., 2018. Holocene Ice-Flow Speedup in the Vicinity of the South Pole. *Geophys. Res. Lett.* 45, 6557–6565. <https://doi.org/10.1029/2018GL078253>
- Lilien, D.A., Hills, B.H., Driscoll, J., Jacobel, R., Christianson, K., 2020. ImpDAR: An open-source impulse radar processor. *Ann. Glaciol.* 61, 114–123. <https://doi.org/10.1017/aog.2020.44>
- Lliboutry, L., 1979. A critical review of analytical approximate solutions for steady state velocities and temperatures in cold ice-sheets. *Gletscherkd. Glazialgeol.* 15, 135–148.
- Lliboutry, L., 1968. General Theory of Subglacial Cavitation and Sliding of Temperate Glaciers. *J. Glaciol.* 7, 21–58.
<https://doi.org/10.1017/S0022143000020396>
- MacGregor, J.A., Fahnestock, M.A., Catania, G.A., Paden, J.D., Gogineni, S.P., Young, S.K., Rybarski, S.C., Mabrey, A.N., Wagman, B.M., Morlighem, M., 2015a. Radiostratigraphy and age structure of the Greenland Ice Sheet. *J. Geophys. Res. Earth Surf.* 120, 212–241. <https://doi.org/10.1002/2014JF003215>.Received
- MacGregor, J.A., Li, J., Paden, J.D., Catania, G. a, Clow, G.D., Fahnestock, M. a, Gogineni, S.P., Grimm, R.E., Morlighem, M., Nandi, S., Seroussi, H., Stillman, D.E., 2015b. Radar attenuation and temperature within the Greenland Ice Sheet. *J. Geophys. Res. Earth Surf.* 120, 983–1008. <https://doi.org/10.1002/2014JF003418>
- MacGregor, J.A., Winebrenner, D.P., Conway, H., Matsuoka, K., Mayewski, P.A., Clow, G.D., 2007. Modeling englacial radar attenuation at Siple Dome, West Antarctica, using ice chemistry and temperature data. *J. Geophys. Res. Earth Surf.* 112, 1–14. <https://doi.org/10.1029/2006JF000717>
- Matsuoka, K., Wilen, L., Hurley, S.P., Raymond, C.F., 2009. Effects of birefringence within ice sheets on obliquely propagating radio waves. *IEEE Trans. Geosci. Remote Sens.* 47, 1429–1443.
<https://doi.org/10.1109/TGRS.2008.2005201>

- Meyer, C.R., Minchew, B.M., 2018. Temperate ice in the shear margins of the Antarctic Ice Sheet: Controlling processes and preliminary locations. *Earth Planet. Sci. Lett.* 498, 17–26. <https://doi.org/10.1016/j.epsl.2018.06.028>
- Mouginot, J., Rignot, E., Scheuchl, B., 2019. Continent-Wide, Interferometric SAR Phase, Mapping of Antarctic Ice Velocity. *Geophys. Res. Lett.* 46, 9710–9718. <https://doi.org/10.1029/2019GL083826>
- Nicholls, K.W., Corr, H.F.J., Stewart, C.L., Lok, L.B., Brennan, P. V., Vaughan, D.G., 2015. Instruments and methods: A ground-based radar for measuring vertical strain rates and time-varying basal melt rates in ice sheets and shelves. *J. Glaciol.* 61, 1079–1087. <https://doi.org/10.3189/2015JoG15J073>
- Perol, T., Rice, J.R., 2015. Shear heating and weakening of the margins of Western Antarctic ice streams. *Geophys. Res. Lett.* 42, 3406–3413. <https://doi.org/10.1002/2015GL063638>. Received
- Peters, L.E., Anandakrishnan, S., Holland, C.W., Horgan, H.J., Blankenship, D.D., Voigt, D.E., 2008. Seismic detection of a subglacial lake near the South Pole , Antarctica. *Geophys. Res. Lett.* 35, 1–5. <https://doi.org/10.1029/2008GL035704>
- Phillips, T., Rajaram, H., Steffen, K., 2010. Cryo-hydrologic warming: A potential mechanism for rapid thermal response of ice sheets. *Geophys. Res. Lett.* 37, 1–5. <https://doi.org/10.1029/2010GL044397>
- Price, P.B., Nagornov, O. V., Bay, R., Chirkin, D., He, Y., Miocinovic, P., Richards, A., Woschnagg, K., Koci, B., Zagorodnov, V., 2002. Temperature profile for glacial ice at the South Pole : Implications for life in a nearby subglacial lake. *Proc. Natl. Acad. Sci.* 99, 7844–7847. <https://doi.org/10.1073/pnas.082238999>
- Raymond, C.F., 1983. Deformation in the vicinity of ice divides. *J. Glaciol.* 29, 357–373. <https://doi.org/10.3189/S0022143000030288>
- Rignot, E., Jacobs, S., Mouginot, J., Scheuchl, B., 2013. Ice-shelf melting around antarctica. *Science (80-.).* 341, 266–270. <https://doi.org/10.1126/science.1235798>
- Robin, G. de Q., 1955. Ice movement and temperature distribution in glaciers and ice sheets. *J. Glaciol.* 2, 523–532.
- Schroeder, D.M., Seroussi, H., Chu, W., Young, D.A., 2016. Adaptively constraining radar attenuation and temperature across the Thwaites Glacier catchment using bed echoes. *J. Glaciol.* 62, 1075–1082. <https://doi.org/10.1017/jog.2016.100>
- Shoji, H., Langway, C.C., 1988. Flow-Law Parameters of the Dye 3, Greenland, Deep Ice Core. *Ann. Glaciol.* 10, 146–150. <https://doi.org/10.3189/s026030550000433x>
- Smith, E.C., Baird, A.F., Kendall, J.M., Martín, C., White, R.S., Brisbourne, A.M., Smith, A.M., 2017. Ice fabric in an Antarctic ice stream interpreted from seismic anisotropy. *Geophys. Res. Lett.* 44, 3710–3718. <https://doi.org/10.1002/2016GL072093>
- Steig, E.J., Huybers, K., Singh, H.A., Steiger, N.J., Ding, Q., Frierson, D.M.W., Popp, T., White, J.W.C., 2015. Influence of West Antarctic Ice Sheet collapse on Antarctic surface climate. <https://doi.org/10.1002/2015GL063861>. Abstract
- Suckale, J., Platt, J.D., Perol, T., Rice, J.R., 2014. Earth Surface Deformation-induced melting in the margins of the West Antarctic ice streams. *J. Geophys. Res. Earth Surf.* 119, 1004–1025. <https://doi.org/10.1002/2013JF003008>. Flow
- Venturelli, R.A., Siegfried, M.R., Roush, K.A., Li, W., Burnett, J., Zook, R., Fricker, H.A., Priscu, J.C., Leventer, A., Rosenheim, B.E., 2020. Mid-Holocene Grounding Line Retreat and Readvance at Whillans Ice Stream, West Antarctica. *Geophys. Res. Lett.* 47. <https://doi.org/10.1029/2020GL088476>
- Weertman, J., 1968. Comparison between Measured and Theoretical Temperature Profiles of the Camp Century, Greenland, Borehole. *J. Geophys. Res.* 73, 2691–2700. <https://doi.org/10.1029/JB073i008p02691>
- Weertman, J., 1957. On the sliding of glaciers. *J. Glaciol.* 3, 33–38. <https://doi.org/10.3189/S002214300002470>
- Welch, B.C., Jacobel, R.W., 2005. Bedrock topography and wind erosion sites in East Antarctica: Observations from the 2002 US-ITASE traverse. *Ann. Glaciol.* 41, 92–96. <https://doi.org/10.3189/172756405781813258>
- Young, T.J., Martín, C., Christoffersen, P., Schroeder, D.M., Tulaczyk, S.M., Dawson, E.J., 2021. Rapid and accurate polarimetric radar measurements of ice crystal fabric orientation at the Western Antarctic Ice Sheet (WAIS) Divide ice core site. *Cryosphere* 15, 4117–4133. <https://doi.org/10.5194/tc-15-4117-2021>